Elena Czeizler | Andrzej Mizera | Ion Petre

A Boolean approach for disentangling the numerical contribution of modules to the system-level behavior of a biomodel

Turku Centre *for* Computer Science

TUCS Technical Report
No 997, January 2011

A Boolean approach for disentangling the numerical contribution of modules to the system-level behavior of a biomodel

Elena Czeizler
Department of Information Technologies, Åbo Akademi University,
FI-20520 Turku, Finland
University of Helsinki, Computational Systems Biology group, Biomedicum,
FI-00014 Helsinki, Finland
elena.czeizler@helsinki.fi

Andrzej Mizera
Department of Information Technologies, Åbo Akademi University,
FI-20520 Turku, Finland
amizera@abo.fi

Ion Petre
Department of Information Technologies, Åbo Akademi University,
FI-20520 Turku, Finland
ipetre@abo.fi

TUCS Technical Report
No 997, January 2011

Abstract

To disentangle the numerical contribution of modules to the system-level behavior of a given biomodel, one often considers knockdown mutant models, investigating the change in the model behavior when modules are systematically included and excluded from the model architecture in all possible ways. We propose in this paper a Boolean logic-based approach for extracting conclusions about the role of each module from the systematic comparison of the numerical behavior of all knockdown mutants. We associate a Boolean variable to each module, expressing when the module is included in the architecture (value 'true') and when it is not (value 'false'). We can then express the satisfiability of system-level properties of the full model, such as efficiency, or economical use of resources, in terms of a Boolean formula expressing in a compact way which model architectures, i.e., which combinations of modules, give rise to the desired property. We demonstrate this methodology on a recently proposed computational model for the heat shock response in eukaryotes. We describe the contribution of each of its three feedback loops towards achieving an economical and effective heat shock response. The applicability of our approach is more general: the same method could be applied to describe how properties of a *wet-lab* biomodel emerge from the combination of its modules. In this case, one would simply replace the numerical simulation of the computational models with the experimental measurement of the behavior of the wet-lab biomodel and that of its knockdown mutant variants.

Keywords: mathematical model — modularization — Boolean logic — heat shock response

TUCS Laboratory
Computational Biomodelling

1 Introduction

Modularization of biomodels There is a sustained experimental and computational effort nowadays towards building large, system-level models for biochemical processes, including regulatory networks, signaling pathways, metabolic pathways, etc. Models can encompass thousands of reactants and reactions, see [7]. On this scale, understanding the details of the network, especially its regulatory mechanisms, becomes a considerable challenge. Similar problems have also been encountered in engineering (and elsewhere), see [9]. Thus, one strategy for elucidating the structure of a biological system, is to adapt to systems biology methods coming from engineering sciences, in particular from control theory, [19, 33, 35]. Applying a control-theoretical analysis to a biological system can provide a systematic way to identify the main regulatory components of a biological system, including its feedforward and feedback mechanisms, see [11]. This, in turn, contributes to the understanding of the reactivity, robustness and efficiency of the biological system. To disentangle the individual contribution of the various components to the network, knockdown mutants are often useful to consider, see [11]. The mutants are numerically compared to each other and to the reference model in an effort to extract the individual contribution of each mechanism to the overall behavior of the system.

Our approach for comparing knockdown mutant models We propose in this paper a novel approach for identifying the numerical contribution of a component to the system-level behavior of a larger model. The core technique we use throughout the paper is to associate a Boolean variable to each of the components. For each knockdown mutant we write a Boolean formula describing the presence or the absence of each component (using the conjunction and the negation of Boolean variables). The obtained Boolean formulas encompass properties of the architecture of the knockdown mutant models. Moreover, these formulas do not depend on the parameters of the models. Going one step further, we can also write a Boolean formula characterizing all mutant architectures that exhibit a given property: we select all knockdown mutants that exhibit that property and construct the disjunction of their Boolean formulas. The formula thus obtained describes which components must be present/absent and in which configurations in order for the system to exhibit the desired property. Iterating this technique for several well chosen systemic properties may help to identify (at least qualitatively) the roles of each component. However, in order to perform numerical simulations for the knockdown mutants, we need to fix a numerical setup for each model, i.e., particular values for both the initial distribution of each species and the kinetic rate constants of the models. In Section 4 we discuss in more details the dependency of our analysis on the numerical setups chosen for the knockdown mutant models.

Our approach is essentially different from the Boolean network framework

often used for qualitative modeling and analysis of biological systems, see, e.g., [6, 17, 18, 32]. Within this framework, one usually associates to each species a Boolean variable, which assumes the value 1 if that particular species is active, i.e., its activity is biologically detectable, or 0 otherwise. Then, Boolean functions are used to update the values of the variables at any time point, depending on the values from the previous time step. Model checking techniques are also often used for querying and validating various models of biomolecular systems, for instance when verifying whether they fulfill a given property expressed as a logical formula, see e.g., [4], [5], [25]. However, in our approach we are more interested in the reverse situation, i.e., to construct the logical formula describing the architecture of those models that verify a given property.

Case study: The eukaryotic heat shock response The heat shock response (HSR) is an evolutionary-conserved global regulatory network found in virtually all living cells. It allows the cell to quickly react to elevated temperatures by the induction of some proteins called *heat shock proteins* (hsp). Exposure to raised temperature leads to protein misfolding, which then accumulate and form aggregates with disastrous effect for the cell. Stress conditions can be caused not only by increased temperature but also by other forms of environmental, chemical or physical stress, such as addition of ethanol, heavy metals, pollutants, high osmolarity, starvation, etc. The heat shock proteins act as chaperones – they stabilize proteins and help to refold the denatured ones. They maintain the proper functioning of the cell by preventing the formation of cytotoxic aggregates.

The heat shock response has been subject to intense scrutiny, see e.g., [8], [28], [34], for at least two main reasons. First, as a primordial, very well-conserved mechanism it is considered a promising candidate for providing insight into the design principles of regulatory networks in general, see e.g., [23], [11]. Second, the heat shock proteins, which are the main actors of the HSR, play crucial role also in many other fundamental cellular processes, see e.g., [16], [27]. Therefore, it is believed that the profound understanding of this defence mechanism would have far-reaching ramifications for the biology of the living cell.

We use as a case study in this paper a model for the heat shock response introduced in [26]. We take a control-based approach to identify three feedback mechanisms in this model. We then apply our Boolean approach for knockdown mutant comparison to identify the contribution of each of the three feedbacks to having a response where the level of misfolded proteins remains low, with a relatively low cost in terms of transactivating the heat shock protein genes.

2 Models

2.1 The eukaryotic heat shock response: a molecular model.

The central role in the heat shock response is played by the *heat shock proteins* (hsp), which act as chaperones for the *misfolded proteins* (mfp) by forming hsp: mfp complexes and helping them to refold. In the model presented in [26], the regulation of the heat shock response is done by controlling the transactivation of the hsp-encoding genes. The transcription of these genes is initiated by some specific proteins called *heat shock factors* (hsf) that first dimerize (hsf_2), then trimerize (hsf_3) to finally bind to the promoters of the hsp-encoding genes, called *heat shock elements* (hse). After the trimers bind to the promoter sites (hsf_3: hse) the transcription and translation of the hsp-encoding genes starts, ultimately producing new hsp molecules.

Once the level of hsp molecules is high enough, the transcription process is turned off through a self-regulating mechanism. The hsp molecules sequestrate the heat shock factors (hsp: hsf), thus preventing them to trimerize and bind to the heat shock elements. The sequestration of the heat shock factors by the heat shock proteins can be done in three different ways: by binding to free hsf, by breaking dimers and trimers, and by unbinding hsf_3 from the DNA promoter sites with simultaneous breaking of the trimer. Once the temperature increases, some of the proteins (prot) start to misfold, driving hsp away from hsf. Thus, the heat shock response is quickly switched on since the heat shock factors are again free and able to promote the synthesis of more heat shock proteins. The reaction rules of the molecular model introduced in [26] are presented in Table 1.

Clearly, the model in Table 1 is very generic in nature. For instance, the protein synthesis and degradation (i.e., reactions 4 and 9) are greatly simplified. Also, although there exist several types of slightly different heat shock proteins, see [14], here they are all treated uniformly, with hsp 70 as base denominator. This is also the case for the heat shock factors and the heat shock elements. Furthermore, in this model all proteins are treated generically, through the prism of whether they are properly folded (prot), or misfolded (mfp). Nevertheless, the model is well suited for the purpose of demonstrating our method for knockdown mutant analysis: the formal results of the analysis can be easily related to an intuitive understanding of the model.

The model in Table 1 includes three mass conservation relations, see [26], for the total amount of hsf, the total amount of proteins (other than hsp and hsf) in the model, as well as for the total amount of hse:

$$[\mathsf{hsf}] + 2 \times [\mathsf{hsf}_2] + 3 \times [\mathsf{hsf}_3] + 3 \times [\mathsf{hsf}_3\colon \mathsf{hse}] + [\mathsf{hsp}\colon \mathsf{hsf}] = C_1,$$

$$[\mathsf{prot}] + [\mathsf{mfp}] + [\mathsf{hsp}\colon \mathsf{mfp}] = C_2,$$

$$[\mathsf{hse}] + [\mathsf{hsf}_3\colon \mathsf{hse}] = C_3,$$

for some mass constants C_1, C_2, C_3.

2.2 The mathematical model.

We associate with the molecular model in Table 1 a mathematical model in terms of ordinary differential equations (ODE), where for each reaction we assume the principle of mass action, see, e.g., [22]. We associate with each reactant a continuous, time-dependant variable that gives its concentration level. For each variable, its differential equation gives the cumulated consumption and production rates of the reactant corresponding to it in the molecular model. Thus, the dynamic behavior of the molecular model is described through the set of all resulting differential equations. We list them in Table 2 and refer to [26] for more details. The estimation of both the kinetic rate constants and the initial values of all reactants was done in [26] by imposing the following three conditions:

(i) The system is in a steady state at $37°C$, i.e., all differential equations are made equal to zero. This condition comes as a natural consequence of the fact that in the absence of the heat shock, i.e., at $37°C$, the model should exhibit no response.

(ii) At $42°C$, the numerical predictions of the model for $[\mathsf{hsf_3}\colon \mathsf{hse}](t)$ should be in agreement with the experimental data from [20].

(iii) At $42°C$, the numerical prediction of the model for $[\mathsf{hsp}](t)$ should verify the data obtained in [26] through a de-novo fluorescent reporter-based experiment.

The kinetic rate constants and the initial values obtained in [26] are presented in Table 3. For more details on the parameter estimation and the experimental validation of the model, we refer to [26]. The resulting model exhibits four major numerical achievements, see [26]:

(A) *It uses economically the cellular resources:* In the absence of heat shock, the transcription of the hsp-encoding gene is almost non-existent. This gene is transactivated only for a short period of time after the temperature increases.

(B) *It is fast to respond to a heat shock:* Upon temperature upshift, the hsp-encoding gene is quickly activated.

(C) *The response is effective:* The level of mfp is kept low when the heat shock is mild.

(D) *The response is scalable:* The cell exhibits a higher response when exposed to higher temperature.

2.3 A control-based modularization of the heat shock response model.

A control-driven analysis of the heat shock response model of [26] was introduced in [10] to decompose the heat shock response model. The model was divided into the following submodules: *the plant*, i.e., the process to be regulated, *the controller*, i.e., the decision-making module, and *the actuator*, i.e., the module which modifies the current state of the system, thus influencing the activity of the plant. A *sensor* which measures the current state of the system and sends this information to the controller and three *feedback mechanisms* regulating this process were also identified. This decomposition of the heat shock model is presented in Table 4, where the reaction numbers refer to the reactions in Table 1.

For a more intuitive understanding of this modularization, we also include a graphical illustration in Figure 1. The three identified feedback loops and their points of interaction with the mainstream process are depicted in Figure 2.

2.4 Knockdown mutant models.

In order to disentangle the role of the feedback mechanisms within the full model, we consider eight knockdown mutants obtained by eliminating from the basic model all combinations of the feedbacks FB_1, FB_2, and FB_3. We will denote each of these mutants as M_X, where $X \subseteq \{1, 2, 3\}$ represents the set of indexes of the feedbacks included in the model M_X:

- M_0 includes no feedback, i.e., it consists of reactions [$\mathbf{r1}$]-[$\mathbf{r4}$], [$\mathbf{r9}$]-[$\mathbf{r12}$] and the backward direction of reaction [$\mathbf{r5}$]. In the control-theory terminology, this model is called the *open-loop design*.
- M_1 includes feedback FB_1, i.e., it consists of reactions [$\mathbf{r1}$]-[$\mathbf{r5}$], [$\mathbf{r9}$]-[$\mathbf{r12}$].
- M_2 includes feedback FB_2, i.e., it consists of reactions [$\mathbf{r1}$]-[$\mathbf{r4}$], [$\mathbf{r6}$]-[$\mathbf{r7}$], [$\mathbf{r9}$]-[$\mathbf{r12}$], and the backward direction of reaction [$\mathbf{r5}$].
- M_3 includes feedback FB_3, i.e., it consists of reactions [$\mathbf{r1}$]-[$\mathbf{r4}$], [$\mathbf{r8}$]-[$\mathbf{r12}$], and the backward direction of reaction [$\mathbf{r5}$].
- $M_{1,2}$ includes feedbacks FB_1, FB_2, i.e., it consists of reactions [$\mathbf{r1}$]-[$\mathbf{r7}$], [$\mathbf{r9}$]-[$\mathbf{r12}$].
- $M_{1,3}$ includes feedbacks FB_1, FB_3, i.e., it consists of reactions [$\mathbf{r1}$]-[$\mathbf{r5}$], [$\mathbf{r8}$]-[$\mathbf{r12}$].
- $M_{2,3}$ includes feedbacks FB_2, FB_3, i.e., it consists of reactions [$\mathbf{r1}$]-[$\mathbf{r4}$], [$\mathbf{r6}$]-[$\mathbf{r12}$], and the backward direction of reaction [$\mathbf{r5}$].
- $M_{1,2,3}$ is the full, reference model, consisting of reactions [$\mathbf{r1}$]-[$\mathbf{r12}$].

To identify the individual contributions of the three feedback mechanisms, we compare the dynamics of these eight models at $42°C$. We choose this temperature since at $42°C$ the experimental data shows a heat shock response both in terms of increased level of misfolded proteins and in terms of transcription activity of the hsp-encoding genes, see [26].

2.5 Numerical setup of the knockdown mutant models.

In our comparison of the numerical knockdown mutant models we aim to focus on the differences stemming from the intrinsic dissimilarities in their architectures and eliminate as much as possible differences coming from unfavorable numerical setups chosen for the various models. For example, we consider all knockdown mutants as viable alternatives for the heat shock response model. We impose the following three constraints:

(1) The kinetic rate constants for the reactions of each of the eight knockdown mutants should be chosen in such a way that the numerical prediction for the time evolution of the level of hsf_3: hse fits in with the experimental data given in [21] on DNA binding of hsf_3.

(2) The initial distribution of the reactants of each mutant should be chosen in such a way that they form a steady state at $37°C$ for that particular model.

(3) For all knockdown mutants, the values of the mass constants C_1, C_2, C_3 are chosen to be identical to those of the reference model $M_{1,2,3}$.

All three constraints come as natural consequences of the fact that we consider all knockdown mutants as viable alternatives for the heat shock model. As such, their dynamic behavior should be in agreement with the existent experimental data and, at the same time, they should be in a steady state in the absence of a heat shock, i.e., at $37°C$. Moreover, since they are all models for the same biological process, they should all assume the same values for the mass constants.

3 Results

When comparing the performance of the eight alternative models we focused on two aspects: the total amount of hsp and the total amount of mfp both at $37°C$ and at $42°C$. We were interested mainly in these two aspects since a very high level of mfp indicates a non-effective response while a very high level of hsp indicates a non-economical response.

We associated to each of the three feedback mechanisms a Boolean variable, denoted by F_1, F_2 and F_3, respectively. Then, for each knockdown mutant we wrote a Boolean formula expressing which of the feedback mechanisms are present in the model, see Table 5 where we denoted by $\wedge$ the conjunction operator

and by $\overline{F_i}$ the negation of the variable F_i. For example, to knockdown mutant $M_{1,2}$ we associated the Boolean formula $F_1 \wedge F_2 \wedge \overline{F_3}$ to express that feedbacks FB_1, FB_2 are included in the model, while FB_3 is not.

Going one step further in our approach, we considered all knockdown mutant models having 'low' total amount of hsp at $37°C$ and at $42°C$, respectively. By writing the disjunction, denoted by $\vee$, of the formulas corresponding to these mutants we obtained a Boolean formula describing the contribution of each feedback to achieving the property: which feedbacks must be present in the model in order for it to exhibit the desired property. We applied the same technique to describe the architectures which exhibit 'low' levels for the total amount of mfp at $37°C$ or at $42°C$.

3.1 Numerical analysis of the knockdown mutant models.

We start our analysis with the mutant M_0, which does not include any of the three feedback mechanisms. The ODE mass-action model associated to M_0 shows that if the mutant starts from its steady state at $37°C$, then at any temperature the differentials for [hsf], [hsf_2], [hsf_3], [hsf_3: hse], [hse] and [hsp: hsf] are zero. That is, those functions remain constant at their steady state values independent of temperature. In particular, the DNA binding level, i.e., hsf_3: hse, remains constant even when we increase the temperature. So, for no numerical setup, this mutant can provide numerical predictions in agreement with the data from [21] if it starts from its steady state at $37°C$. Thus, we discarded this knockdown mutant from our considerations.

For each of the mutants M_1, M_2, M_3, $M_{1,2}$, $M_{1,3}$, and $M_{2,3}$ we performed parameter estimation to identify a numerical setup, i.e., a set of values for the kinetic rate constants, that provides numerical predictions in accordance with the experimental data of [21]. The results are shown in Table 6-A. We then numerically estimated the steady state of each model at $37°C$; the results are given in Table 6-B. Finally, we numerically integrated the mathematical model corresponding to each knockdown mutant starting from its own steady state values in Table 6-B. We integrated the ODEs up to 14400 seconds (in model time), for a temperature value of $42°C$. We collected in Table 7 the maximal values for the total amount of hsp and mfp in each of these models, both at $37°C$ and at $42°C$. For the numerical integration we used the software COPASI [15].

We chose empirically four numerical thresholds separating the 'low' and 'high' values for the total amount of: (i) hsp proteins at $37°C$; (ii) mfp proteins at $37°C$; (iii) hsp proteins at $42°C$; and (iv) mfp proteins at $42°C$. The thresholds we selected were the following: $l^{37}_{\mathsf{hsp}} = 8000$, $l^{37}_{\mathsf{mfp}} = 3000$, $l^{42}_{\mathsf{hsp}} = 8 \times 10^4$, and $l^{42}_{\mathsf{mfp}} = 2.5 \times 10^6$, respectively, all in terms of number of molecules. We plotted the behavior of each knockdown mutant model with respect to these thresholds in Figures 3 and 4.

We considered the following four properties:

- *Property P_1: Low level for the total amount of* hsp *at* $37°C$. This property is exhibited only by the mutants M_1, M_3, $M_{1,2}$, $M_{1,3}$, and $M_{1,2,3}$. Using the Boolean formulas in Table 3 expressing each mutant in terms of their feedback structure, we constructed a Boolean formula for property P_1. This is easily obtained as a disjunctive formula (logical OR) among the Boolean formulas for M_1, M_3, $M_{1,2}$, $M_{1,3}$, and $M_{1,2,3}$:

$$(F_1 \wedge \overline{F_2} \wedge \overline{F_3}) \vee (\overline{F_1} \wedge \overline{F_2} \wedge F_3) \vee (F_1 \wedge F_2 \wedge \overline{F_3}) \vee \\ \vee (F_1 \wedge \overline{F_2} \wedge F_3) \vee (F_1 \wedge F_2 \wedge F_3),$$

  which can be rewritten in a compact form as:

$$F_1 \vee (\overline{F_1} \wedge \overline{F_2} \wedge F_3). \tag{1}$$

  Thus, property P_1 can be satisfied if and only if either feedback FB_1 is present (regardless of whether FB_2 and FB_3 are included or not) or feedback FB_3 is present while feedbacks FB_1 and FB_2 are absent.

- *Property P_2: Low level for the maximal value of the total amount of* hsp *at* $42°C$. This property is exhibited again only by mutants M_1, M_3, $M_{1,2}$, $M_{1,3}$, and $M_{1,2,3}$. So, we obtained the Boolean formula

$$F_1 \vee (\overline{F_1} \wedge \overline{F_2} \wedge F_3). \tag{2}$$

- *Property P_3: Low level for the total amount of* mfp *at* $37°C$. This property is exhibited only by the mutants M_1, M_3, and $M_{1,2,3}$. So, in this case we obtained the Boolean formula

$$(F_1 \wedge \overline{F_2} \wedge \overline{F_3}) \vee (\overline{F_1} \wedge \overline{F_2} \wedge F_3) \vee (F_1 \wedge F_2 \wedge F_3). \tag{3}$$

- *Property P_4: Low level for the maximal value of the total amount of* mfp *at* $42°C$. This property is exhibited by the mutants M_1, M_2, $M_{1,2}$, and $M_{1,2,3}$. In this case, we obtained the Boolean formula

$$(F_1 \wedge \overline{F_3}) \vee (F_1 \wedge F_2 \wedge F_3) \vee (\overline{F_1} \wedge F_2 \wedge \overline{F_3}). \tag{4}$$

Notice that when defining the properties P_1 and P_3, we consider the total amounts of hsp and mfp without referring to the maximal values, as in the case of P_2 or P_4. This is due to the fact that P_1 and P_3 are considered at $37°C$, a temperature at which the system is in a steady state. Thus, the total amounts are not changing in time.

To investigate which knockdown mutants can be both effective and economic, we looked at the models that exhibit low levels for both hsp and mfp. For a temperature of $37°C$, we considered the models that verify simultaneously properties

P_1 and P_3. The Boolean formula describing these architectures was easily obtained as a conjunctive formula (logical AND) among the formulas for properties P_1 and P_3, which could then be rewritten in a compact form as

$$(F_1 \wedge \overline{F_2} \wedge \overline{F_3}) \vee (\overline{F_1} \wedge \overline{F_2} \wedge F_3) \vee (F_1 \wedge F_2 \wedge F_3).$$

Since this was identical with (3), we concluded that at $37°C$, once a mutant achieved a low level for the total amount of mfp, it would also exhibit a low level for the total amount of hsp. For the similar analysis at $42°C$ we were interested in the models that verify simultaneously properties P_2 and P_4. In this case, the Boolean formula describing these architectures is

$$F_1 \wedge (F_2 \vee (\overline{F_2} \wedge \overline{F_3})).$$

This shows that to obtain low values for both hsp and mfp at $42°C$ the first feedback is essential. Moreover, only two types of mutant architectures predicted this outcome: if both FB_1 and FB_2 were present in the model (regardless of whether FB_3 is included or not), or if FB_1 was included while FB_2 and FB_3 were not. Furthermore, it showed that the second feedback, in addition to the first one, has a role in decreasing the levels of both hsp and mfp at $42°C$. The second type of architecture, i.e., when FB_1 was present in the model while FB_2 and FB_3 were absent, showed that the first feedback alone is sufficient to ensure a low enough level of both hsp and mfp at $42°C$. However, when we compared the values predicted by M_1 and $M_{1,2,3}$, see Figure 4, we noticed that the cumulative effect of the second and the third feedbacks added to the first one is to further reduce the total level of mfp.

We noticed that the Boolean formulas corresponding to properties P_1 and P_2 were identical. This means that once a knockdown mutant is able to keep a low level of hsp at $37°C$, it will also be able to respond to heat shock with a relatively low level of hsp. Moreover, this was the case only for two types of mutant architectures: either when the feedback FB_1 was present (regardless of whether FB_2 and FB_3 were included or not) or when feedback FB_3 was present while feedbacks FB_1 and FB_2 were absent. This showed that the first and the third feedbacks have roles in lowering the level of hsp both at $37°C$ and at $42°C$. The first type of mutant architecture, having the feedback FB_1 present, was insensitive to the second and the third feedbacks: whether they were included in the model or not did not change the behavior of the model with respect to P_1 and P_2. The second type of mutant architecture that satisfies the Boolean formula (1) showed that in the absence of the first feedback, the third one is necessary to obtain low levels of hsp both at $37°C$ and at $42°C$.

If, on the other hand, we would require low levels of mfp both at $37°C$ and at $42°C$, i.e., if we would ask for properties P_3 and P_4 to be satisfied, then we would see that the first feedback has to be present in the model. Otherwise, i.e., if $F_1 = 0$, the two Boolean formulas (3) and (4) become $\overline{F_2} \wedge F_3$ and $F_2 \wedge \overline{F_3}$,

respectively, which obviously cannot be simultaneously satisfied. This confirmed again our conclusion that the first feedback is essential for the model to satisfy all four properties P_1, P_2, P_3, and P_4, i.e., for the model to exhibit low levels for both hsp and mfp, both at $37°C$ and at $42°C$.

4 Discussion

4.1 Previous approaches for model comparison.

The technique of mathematically controlled comparison, [31], provides a structured approach for comparing several alternative designs with respect to some chosen measures of functional effectiveness. However, this framework imposes one important constraint on the alternative designs: they are allowed to differ from the reference design in only one component. Moreover, the mathematical models both for the reference design and for the alternative architectures are developed in the framework of canonical nonlinear modeling referred to as S-systems, [29] and [30]. Then, using various systemic properties, one imposes some constraints on all parameters of the alternative designs, setting their values depending on the parameters of the reference model. Finally, one chooses some numerical measures of functional effectiveness and uses them to compare the alternative designs with the reference model. This way, one can determine analytically the qualitative differences between the compared models. If one is also interested in quantifying these differences, then numerical values can be introduced for the parameters of the models. However, by doing this the generality of the results is lost. An extension of the method of mathematically controlled comparison was proposed in [2] to include some statistical methods, see [1] and [3], which allow the use of numerical values for the parameters while still preserving the generality of the conclusions.

Another approach for model comparison was proposed in [10]. Since the alternative designs are submodels of the reference model, the underlying reaction networks of these models are very similar (although not identical), and both the biological constraints and the kinetics of the reactions are taken from the reference model. The only remaining question is how to chose the initial distribution of the variables in the alternative designs. In the mathematically controlled comparison they are usually taken from the reference model, see [11] for a case study using this method. However, this might lead to biased comparisons for some biochemical systems. For instance, for regulatory networks, models should be in a steady state in the absence of the trigger of the response. In particular, the initial values of the reference model are usually chosen in such a way to fulfil this condition. However, this does not imply in general that also a submodel will be in its steady state if it starts from the same initial values as the reference model. As a consequence, the dynamic behavior of the submodel will exhibit two inter-

twined tendencies: the migration from a possible unstable state and the response to a particular stimulus. Thus, if the purpose of the comparison is to determine the efficiency of the response of various submodels to a particular trigger, then the approach proposed in [10] is more appropriate, leading to biologically unbiased results. In this approach, the initial values of the reactants are chosen in such a way that they constitute a steady state of that design in the absence of a trigger. However, also in this approach, the comparison is done locally, for a particular set of parameters. In [24], this method was combined with some statistical methods of [1] and [3], leading to general comparison results independent of the values of the parameters.

4.2 Our approach for knockdown mutant model comparison: advantages and limitations.

In this paper, we proposed a novel approach to the knockdown mutant model comparison problem. First, we associated a Boolean variable to each of the three feedback mechanisms identified in [10] for the reference model of the eukaryotic heat shock response. Then, for each knockdown mutant we wrote a Boolean formula (using the conjunction and negation of the three introduced Boolean variables) characterizing its control architecture, i.e., which of the three feedback mechanisms are present in the model. As such, each of these formulas encompass time-independent properties of the models. This makes our approach very different from the Boolean network framework for modeling biological systems, see [6], [17], [18], [32], where one usually associates a Boolean variable to each species present in the system. Boolean formulas are then used to simulate the time evolution of the species. Moreover, in our approach the Boolean formulas associated to each knockdown mutant are parameter independent, i.e., they are not influenced by the parameters used to describe the compared models. Going one step further, we could introduce a Boolean formula characterizing all those mutant architectures that exhibit a given behavioral property, e.g., low levels of hsp or mfp. This can be easily obtained as a disjunctive formula (logical OR) of the Boolean formulas describing the architectures of the mutants exhibiting the required property. However, in order to perform numerical simulations of the models we needed numerical setups for each of the knockdown mutants, i.e., specific values both for the initial distribution of the reactants and for the kinetic rate constants of the models. For the initial values of the variables, we chose the approach proposed in [10], i.e., we set them separately for each knockdown mutant in such a way that they form a steady state for that particular model. Regarding the kinetic rate constants in each of the knockdown mutants, one approach is to take them from the reference model, see [10]. The idea in this case is to make the whole comparison in the numerical setup of the reference model. Alternatively, we proposed here to separately estimate the kinetic constants of each alternative model with respect to available experimental data. In other words, we considered all models to be vi-

able alternatives for the biological system and, as such, we took for each of them a most favorable numerical setup.

Since the numerical setup giving a good model fit is in general not unique, it means that our analysis is sensitive with respect to the choice of the values for the kinetic constants. This is often the case when model fitting is involved, see [7]. Repeating the analysis for several numerical setups (all of them as good in terms of fitting the model to the experimental data) would enrich the conclusions, by potentially showing that the same model architecture can exhibit different properties depending on the numerical setup. The conclusions of the analysis also depend on the numerical values chosen for the thresholds l^{37}_{hsp}, l^{37}_{mfp}, l^{42}_{hsp}, and l^{42}_{mfp}.

It is crucial for our approach that all knockdown mutant models are considered in the analysis, i.e., all possible combinations ON/OFF of the model components are included in the comparison. In this way, we obtain a complete characterization of the properties being analyzed in terms of *all* model architectures that can exhibit those properties. For a large number of components, this approach becomes quickly computationally challenging: for n components to be analyzed, there are 2^n knockdown mutant models to be compared. Including in the comparison only a part of those mutants is also possible but then the output of the method is partial: one only discovers *some*, potentially not all, model architectures exhibiting the property of interest.

When we compared the numerical behavior of the knockdown mutants, we chose a mathematical model formulation in terms of ordinary differential equations. However, our approach is independent of this formulation and it would work equally well with other formulations, such as continuous-time Markov chains and their numerical simulations based on Gillespie's algorithm, see [12, 13].

Our approach can be easily extended to a more refined analysis, where the range of the properties to be analyzed is divided into more domains than just 'low' and 'high'. The range could in fact be divided into an arbitrarily high number of intermediate domains, depending on the details of the case study. A Boolean formula could be associated to characterize each of those domains in a manner similar to that demonstrated in this paper.

5 Conclusions

We proposed in this paper a computational method to characterize how a system-level behavior emerges from combinations of a network's modules, and what is the contribution of each module to that behavior. In our approach, a system-level property is described as a Boolean formula, where each module is represented through a Boolean variable, having value 'true' only if the module contributes to that system property. We applied this method to a computational, *in-silico* model and for that, we analyzed the numerical properties of this model and of all its knockdown mutants. However, the applicability of our approach is more general.

For example, one could think of applying the same approach in experimental practice in biology. When investigating a functional structure of a *wet-lab* biomodel, one would identify a number of *bio-modules* and design wet-lab knockdown mutants where certain combinations of bio-modules would be removed, switched-off or silenced in some way. The individual mutants would be further experimentally tested for certain properties. Finally, in order to describe how the properties of the wet-lab biomodel emerge from the combination of its bio-modules, one could adapt our method: Boolean variables would represent the bio-modules, Boolean formulas would describe the system-level biological properties and the numerical simulation of the computational models would be replaced with the experimental measurement of the behavior of the wet-lab biomodel and that of its knockdown mutant variants.

6 Acknowledgements

This work was supported by Academy of Finland, grants 129863, 108421, and 122426. Andrzej Mizera is on leave of absence from the Institute of Fundamental Technological Research, Polish Academy of Sciences, Warsaw, Poland.

References

[1] R. Alves and M. A. Savageau. Comparing systemic properties of ensembles of biological networks by graphical and statistical methods. *Bioinformatics*, 16:527–533, 2000.

[2] R. Alves and M. A. Savageau. Extending the method of mathematically controlled comparison to include numerical comparisons. *Bioinformatics*, 16:786–798, 2000.

[3] R. Alves and M. A. Savageau. Systemic properties of ensembles of metabolic networks: application of graphical and statistical methods to simple unbranched pathways. *Bioinformatics*, 16:534–547, 2000.

[4] G. Batt, C. Belta, and R. Weiss. Model checking liveness properties of genetic regulatory networks. In *Proceedings of the International conference on tools and algorithms for the construction and analysis of systems*, 2007.

[5] N. Chabrier and F. Fages. Symbolic model checking of biochemical networks. In *Proceedings of the International Workshop on Computational Methods in Systems Biology*, pages 149–162, 2003.

[6] M. Chaves, R. Albert, and E. D. Sontag. Robustness and fragility of boolean models for genetic regulatory networks. *J Theor Biol*, 235:431–49, 2005.

[7] W. W. Chen, B. Schoeberl, P. J. Jasper, M. Niepel, U. B. Nielsen, D. A. Lauffenburger, and P. K. Sorger. Input-output behavior of erbb signaling pathways as revealed by a mass action model trained against dynamic data. *Molecular Systems Biology*, 5:239, 2009.

[8] Y. Chen, T. S. Voegeli, P. P. Liu, E. G. Noble, and R. W. Currie. Heat shock paradox and a new role of heat shock proteins and their receptors as anti-inflammation targets. *Inflamm Allergy Drug Targets*, 6(2):91–100, 2007.

[9] M. E. Csete and J. C. Doyle. Reverse engineering of biological complexity. *Science*, 295:1664–1669, 2002.

[10] E. Czeizler, E. Czeizler, R.-J. Back, and I. Petre. Control strategies for the regulation of the eukaryotic heat shock response. In P. Degano and R. Gorrieri, editors, *Lecture Notes in Bioinformatics*, volume 5688, pages 111–125. Springer, Berlin, Heidelberg, 2009.

[11] H. El-Samad, H. Kurata, J. C. Doyle, C. A. Gross, and M. Khammash. Surviving heat shock: Control strategies for robustness and performance. *Proc Natl Acad Sci USA*, 102:2736–2741, 2005.

[12] D. T. Gillespie. A general method for numerically simulating the stochastic time evolution of coupled chemical reactions. *J Comput Phys*, 22:403–434, 1976.

[13] D. T. Gillespie. Exact stochastic simulation of coupled chemical reactions. *J Phys Chem*, 81:2340–2361, 1977.

[14] C. Holmberg, S. Tran, J. Eriksson, and L. Sistonen. Multisite phosphorylation provides sophisticated regulation of transcription factors. *Trends Biochem Sci*, 27(12):619–627, 2002.

[15] S. Hoops, S. Sahle, R. Gauges, C. Lee, J. Pahle, N. Simus, M. Singhal, L. Xu, P. Mendes, and U. Kummer. Copasi – a COmplex PAthway SImulator. *Bioinformatics*, 22:3067–3074, 2006.

[16] H. K. Kampinga. Thermotolerance in mammalian cells: protein denaturation and aggregation, and stress proteins. *J. Cell Science*, 104:11–17, 1993.

[17] S. Kauffman, C. Peterson, B. Samuelsson, and C. Troein. Random boolean network models and the yeast transcriptional network. *Proc Natl Acad Sci USA*, 100:14796–14799, 2003.

[18] G. Kervizic and L. Corcos. Dynamical modeling of the cholesterol regulatory pathway with boolean networks. *BMC Systems Biology*, 2:99, 2008.

[19] H. Kitano. Systems biology: A brief overview. *Science*, 295:1662–1664, 2002.

[20] M. Kline and R. Morimoto. Repression of the heat shock factor 1 transcriptional activation domain is modulated by constitutive phosphorylation. *Molecular and Cellular Biology*, 17(4):2107–2115, 1997.

[21] M. P. Kline and R. I. Morimoto. Repression of the heat shock factor 1 transcriptional activation domain is modulated by constitutive phosphorylation. *Molecular and Cellular Biology*, 17:2107–2115, 1997.

[22] E. Klipp, R. Herwig, A. Kowald, C. Wierling, and H. Lehrach. *Systems Biology in Practice. Concepts, Implementation and Application*. Wiley-VCH, Weinheim, 2005.

[23] H. Kurata, H. El-Samad, T. Yi, M. Khamash, and J. Doyle. Feedback regulation of the heat shock response in e.coli. In *Proceedings of the 40th IEEE Conference on Decision and Control*, pages 837–842, 2001.

[24] A. Mizera, E. Czeizler, and I. Petre. Methods for biochemical model decomposition and quantitative submodel comparison. *Israel J Chem*, 51(1):151–164, 2011.

[25] S. Peres and J.-P. Comet. Contribution of computational tree logic to biological regulatory networks: Example from pseudomonas aeruginosa. In *Proceedings of the International Workshop on Computational Methods in Systems Biology*, pages 47 – 56, 2003.

[26] I. Petre, A. Mizera, C. L. Hyder, A. Mikhailov, J. E. Eriksson, L. Sistonen, and R.-J. Back. A simple mass-action model for the eukaryotic heat shock response and its mathematical validation. *Natural Computing*, 10(1):595–612, 2011.

[27] A. G. Pockley. Heat shock proteins as regulators of the immune response. *The Lancet*, 362(9382):469–476, 2003.

[28] M. V. Powers and P. Workman. Inhibitors of the heat shock response: Biology and pharmacology. *FEBS Lett.*, 581(19):3758–3769, 2007.

[29] M. A. Savageau. Biochemical systems analysis: I. Some mathematical properties of the rate law for the component enzymatic reactions. *J Theoret Biol*, 25:365–369, 1969.

[30] M. A. Savageau. Biochemical systems analysis: II. the steady-state solutions for an n-pool system using a power-law approximation. *J Theoret Biol*, 25:370–379, 1969.

[31] M. A. Savageau. The behavior of intact biochemical control systems. *Curr. Top. Cell. Reg.*, 6:63–130, 1972.

[32] I. Shmulevich, R. Dougherty, and W. Zhang. From boolean to probabilistic boolean networks as models of genetic regulatory networks. *Proc IEEE*, 90:1778–1792, 2002.

[33] E. Sontag. Molecular systems biology and control. *European Journal of Control*, 11:396–435, 2005.

[34] R. Voellmy and F. Boellmann. Chaperone regulation of the heat shock protein response. *Adv Exp Med Biol*, 594:89–99, 2007.

[35] O. Wolkenhauer. Systems biology: the reincarnation of systems theory applied in biology? *Briefings in Bioinformatics*, 2:258–270, 2001.

Table 1: The molecular model for the eukaryotic heat shock response proposed in [26].

Reaction	
$2\,\mathsf{hsf} \leftrightarrows \mathsf{hsf}_2$	$[\mathbf{r1}]$
$\mathsf{hsf} + \mathsf{hsf}_2 \leftrightarrows \mathsf{hsf}_3$	$[\mathbf{r2}]$
$\mathsf{hsf}_3 + \mathsf{hse} \leftrightarrows \mathsf{hsf}_3\colon \mathsf{hse}$	$[\mathbf{r3}]$
$\mathsf{hsf}_3\colon \mathsf{hse} \rightarrow \mathsf{hsf}_3\colon \mathsf{hse} + \mathsf{hsp}$	$[\mathbf{r4}]$
$\mathsf{hsp} + \mathsf{hsf} \leftrightarrows \mathsf{hsp}\colon \mathsf{hsf}$	$[\mathbf{r5}]$
$\mathsf{hsp} + \mathsf{hsf}_2 \rightarrow \mathsf{hsp}\colon \mathsf{hsf} + \mathsf{hsf}$	$[\mathbf{r6}]$
$\mathsf{hsp} + \mathsf{hsf}_3 \rightarrow \mathsf{hsp}\colon \mathsf{hsf} + 2\,\mathsf{hsf}$	$[\mathbf{r7}]$
$\mathsf{hsp} + \mathsf{hsf}_3\colon \mathsf{hse} \rightarrow \mathsf{hsp}\colon \mathsf{hsf} + 2\,\mathsf{hsf} + \mathsf{hse}$	$[\mathbf{r8}]$
$\mathsf{hsp} \rightarrow \emptyset$	$[\mathbf{r9}]$
$\mathsf{prot} \rightarrow \mathsf{mfp}$	$[\mathbf{r10}]$
$\mathsf{hsp} + \mathsf{mfp} \leftrightarrows \mathsf{hsp}\colon \mathsf{mfp}$	$[\mathbf{r11}]$
$\mathsf{hsp}\colon \mathsf{mfp} \rightarrow \mathsf{hsp} + \mathsf{prot}$	$[\mathbf{r12}]$

Table 2: The differential equations of the associated mathematical model originally introduced in [26].

Equation	(Equation number)
$d[\mathsf{hsf}]/dt = -2k_1^+[\mathsf{hsf}]^2 + 2k_1^-[\mathsf{hsf}_2] - k_2^+[\mathsf{hsf}][\mathsf{hsf}_2] + k_2^-[\mathsf{hsf}_3] - k_5^+[\mathsf{hsf}][\mathsf{hsp}] + k_5^-[\mathsf{hsp{:}\ hsf}] + k_6[\mathsf{hsf}_2][\mathsf{hsp}] + 2k_7[\mathsf{hsf}_3][\mathsf{hsp}] + 2k_8[\mathsf{hsf_3{:}\ hse}][\mathsf{hsp}]$	(5)
$d[\mathsf{hsf}_2]/dt = k_1^+[\mathsf{hsf}]^2 - k_1^-[\mathsf{hsf}_2] - k_2^+[\mathsf{hsf}][\mathsf{hsf}_2] + k_2^-[\mathsf{hsf}_3] - k_6[\mathsf{hsf}_2][\mathsf{hsp}]$	(6)
$d[\mathsf{hsf}_3]/dt = k_2^+[\mathsf{hsf}][\mathsf{hsf}_2] - k_2^-[\mathsf{hsf}_3] - k_3^+[\mathsf{hsf}_3][\mathsf{hse}] + k_3^-[\mathsf{hsf_3{:}\ hse}] - k_7[\mathsf{hsf}_3][\mathsf{hsp}]$	(7)
$d[\mathsf{hse}]/dt = -k_3^+[\mathsf{hsf}_3][\mathsf{hse}] + k_3^-[\mathsf{hsf_3{:}\ hse}] + k_8[\mathsf{hsf_3{:}\ hse}][\mathsf{hsp}]$	(8)
$d[\mathsf{hsf_3{:}\ hse}]/dt = k_3^+[\mathsf{hsf}_3][\mathsf{hse}] - k_3^-[\mathsf{hsf_3{:}\ hse}] - k_8[\mathsf{hsf_3{:}\ hse}][\mathsf{hsp}]$	(9)
$d[\mathsf{hsp}]/dt = k_4[\mathsf{hsf_3{:}\ hse}] - k_5^+[\mathsf{hsf}][\mathsf{hsp}] + k_5^-[\mathsf{hsp{:}\ hsf}] - k_6[\mathsf{hsf}_2][\mathsf{hsp}] - k_7[\mathsf{hsf}_3][\mathsf{hsp}] - k_8[\mathsf{hsf_3{:}\ hse}][\mathsf{hsp}] - k_{11}^+[\mathsf{hsp}][\mathsf{mfp}] + (k_{11}^- + k_{12})[\mathsf{hsp{:}\ mfp}] - k_9[\mathsf{hsp}]$	(10)
$d[\mathsf{hsp{:}\ hsf}]/dt = k_5^+[\mathsf{hsf}][\mathsf{hsp}] - k_5^-[\mathsf{hsp{:}\ hsf}] + k_6[\mathsf{hsf}_2][\mathsf{hsp}] + k_7[\mathsf{hsf}_3][\mathsf{hsp}] + k_8[\mathsf{hsf_3{:}\ hse}][\mathsf{hsp}]$	(11)
$d[\mathsf{mfp}]/dt = \phi_T[\mathsf{prot}] - k_{11}^+[\mathsf{hsp}][\mathsf{mfp}] + k_{11}^-[\mathsf{hsp{:}\ mfp}]$	(12)
$d[\mathsf{hsp{:}\ mfp}]/dt = k_{11}^+[\mathsf{hsp}][\mathsf{mfp}] - (k_{11}^- + k_{12})[\mathsf{hsp{:}\ mfp}]$	(13)
$d[\mathsf{prot}]/dt = -\phi_T[\mathsf{prot}] + k_{12}[\mathsf{hsp{:}\ mfp}]$	(14)

Table 3: The numerical values of the parameters and the initial values of the variables of the heat shock response model of [26].

A

Param.	Value	Units
k_1^+	3.49	$\frac{ml}{\#\cdot s}$
k_1^-	0.19	s^{-1}
k_2^+	1.07	$\frac{ml}{\#\cdot s}$
k_2^-	10^{-9}	s^{-1}
k_3^+	0.17	$\frac{ml}{\#\cdot s}$
k_3^-	$1.21 \cdot 10^{-6}$	s^{-1}
k_4	$8.3 \cdot 10^{-3}$	s^{-1}
k_5^+	9.74	$\frac{ml}{\#\cdot s}$
k_5^-	3.56	s^{-1}
k_6	2.33	$\frac{ml}{\#\cdot s}$
k_7	$4.31 \cdot 10^{-5}$	$\frac{ml}{\#\cdot s}$
k_8	$2.73 \cdot 10^{-7}$	$\frac{ml}{\#\cdot s}$
k_9	$3.2 \cdot 10^{-5}$	s^{-1}
k_{11}^+	$3.32 \cdot 10^{-3}$	$\frac{ml}{\#\cdot s}$
k_{11}^-	4.44	s^{-1}
k_{12}	13.94	s^{-1}

B

Variable	Initial conc.
[hsf]	0.67
[hsf_2]	$8.7 \cdot 10^{-4}$
[hsf_3]	$1.2 \cdot 10^{-4}$
[hse]	29.73
[hsf_3: hse]	2.96
[hsp]	766.88
[hsp: hsf]	1403.13
[mfp]	517.352
[hsp: mfp]	71.65
[prot]	1.15×10^8

A. The numerical values of the parameters. B. The initial values of all variables.

Table 4: The control-based decomposition of the model in Table 1. We denote the 'left-to-right' direction of reaction $[\mathbf{r5}]$ by $[\mathbf{r5}]^+$ and by $[\mathbf{r5}]^-$ its 'right-to-left' direction.

Module and main task	Reactions
Plant (protein misfolding and refolding)	$[\mathbf{r10}]$, $[\mathbf{r11}]$, $[\mathbf{r12}]$
Actuator (regulate the level of hsp)	$[\mathbf{r4}]$, $[\mathbf{r9}]$
Sensor (measure the level of hsp)	
Controller (modulate level of DNA binding)	$[\mathbf{r1}]$, $[\mathbf{r2}]$, $[\mathbf{r3}]$, $[\mathbf{r5}]^-$
Feedback FB_1 (sequestration of hsf)	$[\mathbf{r5}]^+$
Feedback FB_2 (dimer and trimer breaking)	$[\mathbf{r6}]$, $[\mathbf{r7}]$
Feedback FB_3 (hsp-forced DNA unbinding)	$[\mathbf{r8}]$

Table 5: Boolean formulas encoding the presence or absence of the three feedback mechanisms in each of the eight models.

Mutant	Boolean formula
M_0	$\overline{F_1} \wedge \overline{F_2} \wedge \overline{F_3}$
M_1	$F_1 \wedge \overline{F_2} \wedge \overline{F_3}$
M_2	$\overline{F_1} \wedge F_2 \wedge \overline{F_3}$
M_3	$\overline{F_1} \wedge \overline{F_2} \wedge F_3$
$M_{1,2}$	$F_1 \wedge F_2 \wedge \overline{F_3}$
$M_{1,3}$	$F_1 \wedge \overline{F_2} \wedge F_3$
$M_{2,3}$	$\overline{F_1} \wedge F_2 \wedge F_3$
$M_{1,2,3}$	$F_1 \wedge F_2 \wedge F_3$

Table 6: Numerical values of the parameters and the initial values of the variables of the knockdown mutants. A. The numerical values of the parameters in each of the six knockdown mutants. k_i denotes the kinetic rate constant of the irreversible reaction (i). k_i^+ denotes the 'left-to-right' direction of reaction (i), while k_i^- denotes its 'right-to-left' direction. Notice that there is no parameter k_{10} in the table. It is assumed to be the temperature-dependant parameter ϕ_T whose value is determined from the expression presented and discussed in [26]. B. The initial values of all variables in each of the six knockdown mutants.

A

	M_1	M_2	M_3	$M_{1,2}$	$M_{1,3}$	$M_{2,3}$
k_1^+	0.02	10.00	$4.36 \cdot 10^{-7}$	7.24	0.04	10.00
k_1^-	0.01	9.90	$1.36 \cdot 10^{-7}$	$1.84 \cdot 10^{-5}$	0.26	0.01
k_2^+	9.90	6.02	0.23	0.34	0.00	0.01
k_2^-	0.01	0.01	$1.22 \cdot 10^{-6}$	$1.05 \cdot 10^{-5}$	0.03	$8.04 \cdot 10^{-5}$
k_3^+	0.08	3.04	0.01	0.70	0.13	10.00
k_3^-	0.66	0.00	0.17	0.15	0.00	0.00
k_4	0.01	10.00	0.19	0.00	0.51	1.59
k_5^-	0.00	10.00	9.98	1.23	3.41	10.00
k_5^+	0.15	-	-	10.00	$1.00 \cdot 10^{-9}$	-
k_6	-	0.60	-	$1.00 \cdot 10^{-9}$	-	0.13
k_7	-	0.24	-	10.00	-	$2.08 \cdot 10^{-7}$
k_8	-	-	0.51	-	0.23	3.20
k_9	$3.20 \cdot 10^{-5}$	$3.20 \cdot 10^{-5}$	$3.20 \cdot 10^{-5}$	$3.20 \cdot 10^{-5}$	$3.20 \cdot 10^{-5}$	$3.20 \cdot 10^{-5}$
k_{11}^+	9.75	10.00	0.38	0.00	0.00	0.57
k_{11}^-	6.52	$1.00 \cdot 10^{-9}$	10.00	$1.30 \cdot 10^{-8}$	0.32	5.01
k_{12}	32.08	0.01	0.70	16.47	0.17	0.05

B

	M_1	M_2	M_3	$M_{1,2}$	$M_{1,3}$	$M_{2,3}$
[hsf]	0.03	36.95	1399.68	1.27	67.96	33.45
[hsf_2]	0.00	0.02	0.00	27.33	667.19	130.23
[hsf_3]	0.11	$1.52 \cdot 10^{-5}$	4.28	0.01	2.39	0.09
[hse]	32.28	28.97	32.67	31.41	32.64	32.68
[hsf_3: hse]	0.41	3.72	0.02	1.28	0.05	0.01
[hsp]	99.31	$1.16262 \cdot 10^{6}$	100.05	130.39	839.82	662.90
[hsp: hsf]	1411.09	1364.52	0.09	1352.88	3.00	1118.47
[mfp]	1.24	$8.58 \cdot 10^{-5}$	405.56	47164.90	3915.46	244.61
[hsp: mfp]	31.14	144533	1426.09	60.62	6024.21	18259.40
[prot]	$1.14916 \cdot 10^{8}$	$1.14771 \cdot 10^{8}$	$1.14914 \cdot 10^{8}$	$1.14868 \cdot 10^{8}$	$1.14906 \cdot 10^{8}$	$1.14897 \cdot 10^{8}$

Table 7: a) The numerical values for the total amount of hsp and mfp at $37°C$, b) The maximal numerical values for the total amount of hsp and mfp at $42°C$. All values are in terms of number of molecules and should be interpreted as an average of a population of cells

a)

	Total hsp	Total mfp
M_1	1541	32,3
M_2	$1,3 \times 10^6$	144533
M_3	1526	1832
$M_{1,2}$	1544	47225
$M_{1,3}$	6867	9939,6
$M_{2,3}$	20040,8	18504
$M_{1,2,3}$	2241	589

b)

	Max Total hsp	Max total mfp
M_1	2458	623997
M_2	$2,41 \times 10^6$	$1,28 \times 10^6$
M_3	19782,5	$8,8 \times 10^6$
$M_{1,2}$	1978,6	$2,41 \times 10^6$
$M_{1,3}$	73931,4	$1,3 \times 10^7$
$M_{2,3}$	233778	$1,27 \times 10^7$
$M_{1,2,3}$	3157	16116

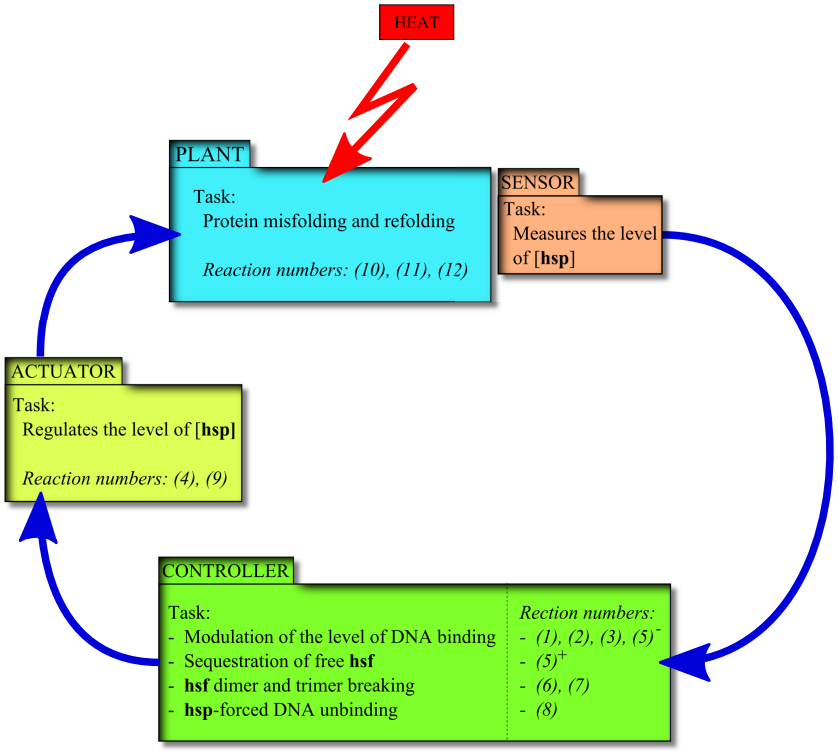

Figure 1: The control structure of the heat shock response network.

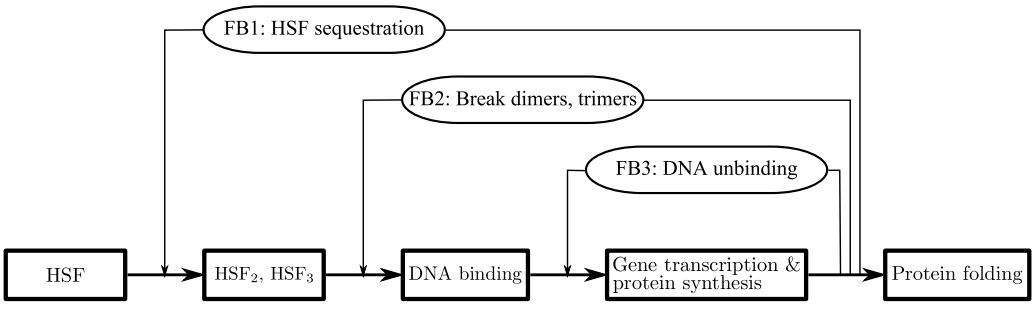

Figure 2: The control structure of the heat shock response network.

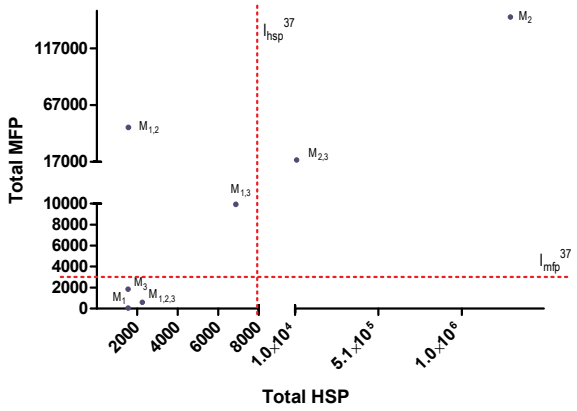

Figure 3: The total amount of hsp and mfp for each of the seven models at $37°C$. Values on the axes are in terms of number of molecules and should be interpreted as an average of a population of cells.

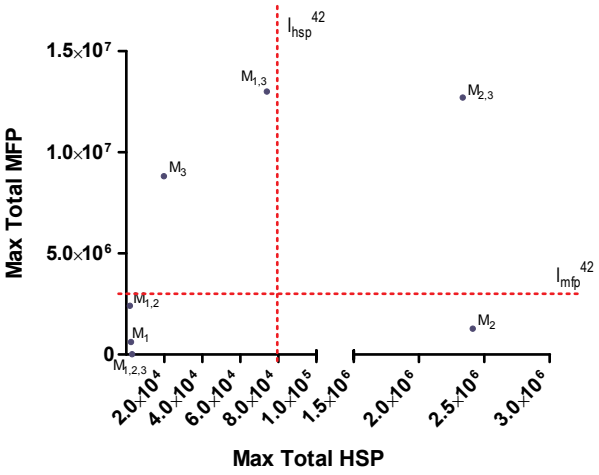

Figure 4: The maximal value for the total amount of hsp and mfp for each of the seven models at $42°C$. Values on the axes are in terms of number of molecules and should be interpreted as an average of a population of cells.

Turku
Centre *for*
Computer
Science

Joukahaisenkatu 3-5 B, FI-20520 Turku, Finland | www.tucs.fi

University of Turku
- Department of Information Technology
- Department of Mathematics

Åbo Akademi University
- Department of Computer Science
- Institute for Advanced Management Systems Research

Turku School of Economics and Business Administration
- Institute of Information Systems Sciences

ISBN 978-952-12-2544-4
ISSN 1239-1891